



## Open Archive Toulouse Archive Ouverte (OATAO)

OATAO is an open access repository that collects the work of Toulouse researchers and makes it freely available over the web where possible.

This is an author-deposited version published in: <http://oatao.univ-toulouse.fr/>  
Eprints ID: 5751

**To link to this article:** DOI:10.1016/J.POWTEC.2010.05.010  
URL: <http://dx.doi.org/10.1016/J.POWTEC.2010.05.010>

**To cite this version:** Isabeta, Nelson and Biscans, Béatrice (2010) Fractal dimension of fumed silica: Comparison of light scattering and electron microscope methods. *Powder Technology*, vol. 203 (n°10). pp. 206-210. ISSN 0032-5910

Any correspondence concerning this service should be sent to the repository administrator: [staff-oatao@listes.diff.inp-toulouse.fr](mailto:staff-oatao@listes.diff.inp-toulouse.fr)

# Fractal dimension of fumed silica: Comparison of light scattering and electron microscope methods

Nelson Ibaseta<sup>1</sup>, Béatrice Biscans\*

Université de Toulouse, Laboratoire de Génie Chimique UMR CNRS 5503, Toulouse, France

## A B S T R A C T

Due to the enormous increase in nanopowder production, it becomes necessary to find and develop adapted characterization techniques. In the case of nanostructured agglomerates, the structure of these particles has a direct impact on flowing, and handling, but also on end-use final product properties. In this work, a fractal approach is used to characterize the agglomerate structure using two different, commercially available and widely used, methods: static light scattering (SLS) and image analysis of scanning electron microscope (SEM) photographs of the aggregates. Fumed silica aggregates are used for this comparison. The results by image analysis show that fumed silica aggregates have a two-level structure, made of compact aggregates of open aggregates of nanoparticles. This structure is not detected by SLS. For such a structure, SLS seems to be less accurate than image analysis method, although it could be an interesting technique in more simple cases, since it is a much less time-consuming technique.

## 1. Introduction

Worldwide production of nanoparticles (particles sizing less than 100 nm, also called ultrafine particles) has undergone a big expansion during the last years. This significant increase comes from the new properties developed by nanoparticles (different from those of the micrometric particles of the same substances), due to their high surface-to-volume ratio. Hence, nanoparticles find several applications in different domains such as for example pharmaceuticals, materials, electronics or catalysis [1]. These applications are strongly dependent on the particle properties, such as size, crystalline and surface properties.

Nanoparticles can exist in liquid suspensions (where they can be electrically or sterically stabilized) or as a powder. In the last case, nanoparticles tend to agglomerate (because of their very reactive surface) leading to form nanostructured powders. Hence, a complete characterization of the powder implies the analysis of the properties of the nanostructured agglomerates, such as agglomerate structure. One possibility to characterize the agglomerate structure is to use the concept of fractal dimension [2].

As reminder, a mathematical fractal is a scale-invariant object, where the fractal dimension,  $D_f$ , is:

$$D_f = \frac{\ln n}{\ln h} \quad (1)$$

where the fractal object is made of  $n$  elements whose size has been reduced by a factor  $h$ . A similar concept can be used for agglomerates, where the number of primary particles that constitute the agglomerate is related to the size of the agglomerate by:

$$D_f = \frac{\ln(n_{pp} / k_0)}{\ln(R_g / a)} \quad (2)$$

where  $a$  is the primary particle radius and  $k_0$  is a coefficient whose value is roughly 1.1.  $R_g$  is a root mean square radius (called radius of gyration), which value is given by:

$$R_g^2 = \frac{\int r^2 \rho(r) \cdot d^3r}{\int \rho(r) \cdot d^3r} \quad (3)$$

where  $\rho(r)$  is the density at location  $r$ .

The fractal dimension allows a quantitative description of the degree of openness, or ramification, of the random aggregate. The fractal dimension of compact aggregates has a value close to 3, whereas chain-like aggregates have a fractal dimension around 1.

\* Corresponding author. Laboratoire de Génie Chimique UMR CNRS 5503, 4, allée Emile Monso BP 84324, Toulouse Cedex 04, France. Tel.: +33 5 34 32 36 38.

E-mail address: [Beatrice.Biscans@ensiacet.fr](mailto:Beatrice.Biscans@ensiacet.fr) (B. Biscans).

<sup>1</sup> Present address: Ecole Centrale Marseille, Laboratoire de Mécanique, Modélisation et Procédés Propres UMR CNRS 6181, Aix en Provence, France.

Eq. (2) is usually rearranged to show that the ratio between the solid fraction and the void fraction is given by:

$$\frac{1-\varepsilon}{\varepsilon} = k_0 \left( \frac{R_g}{a} \right)^{D_f-3} \quad (4)$$

This change in the porosity of the aggregate modifies its effective density as well as the drag force exerted by the air onto the particle. This change implies a variation of aggregate inertia, with further effects on aggregate characterization by settling methods, or powder recovery in cyclones.

Moreover, the fractal dimension determines the coordination number in the aggregate (i.e. the number of primary particles close to a given particle). A small fractal dimension implies a small coordination number, and hence a smaller tensile strength of the aggregate. Aggregates with a small fractal dimension are then easier to disperse in a liquid, but they can liberate more ultrafine particles in the air during the powder handling too [3].

Finally, the fractal dimension modifies the total scattering cross section of the aggregate [4]. Hence, the fractal dimension plays a part in such different phenomena as aggregate settling, strength or light scattering. Powder separation, handling and characterization are then strongly dependent on the fractal dimension of the aggregates. The goal of the present work is to compare two different techniques enabling the characterization of the fractal dimension of a nanostructured powder: static light scattering (SLS) and image analysis of SEM photographs.

## 2. Methods and materials

In the following sections two different methods enabling the measurement of the fractal dimension are presented. The first one concerns the optical characterization of fractal aggregates by SLS, whereas the second one concerns the analysis of projected images (for instance by SEM photographs) of the aggregates. Both methods were tested for fumed silica (Aerosil 200, Degussa) shown in Fig. 1.

### 2.1. Fractal dimension by static light scattering (SLS)

When an incident beam of light illuminates an aggregate, two different types of processes can occur. The aggregate can convert the radiant energy in other forms of energy (e.g. heat), and this process is called absorption. Alternatively, the aggregate can reradiate this energy in the same wave length. This process is called scattering. The reradiation takes place in all directions, but usually with different

intensities in different directions. In SLS, the intensity  $I$  of scattered light is measured at different angles, by placing several transducers at these different angles  $\theta$ . For fractal aggregates, the intensity of the scattered light depends on the scattering angle [4] according to Eq. (5), where  $q$  is the scattering wave vector, given by Eq. (6).

$$S(q) = \begin{cases} 1 & \text{for } qR_g \ll 1 \\ 1 - \frac{1}{3} q^2 R_g^2 & \text{for } qR_g \approx 1 \\ CC_p (qR_g)^{-D_f} & \text{for } qR_g \gg 1 \end{cases} \quad (5)$$

$S(q)$  is the intensity  $I$  of the scattered light at the angle  $\theta$ , normalized by the intensity of the scattered light  $I(0)$  for  $\theta \approx 0$ .  $S(q)$  is called the structure factor.

$$q = \frac{4\pi}{\lambda} \sin\left(\frac{\theta}{2}\right) \quad (6)$$

Hence, at small  $q$  ( $\theta \approx 0$ ), the scattering is constant and proportional to the product of the total number of primary particles and the total number of aggregates in the volume cell. The suspension of particles is seen as a whole. This is termed the Rayleigh regime. For high values of  $q$  ( $qR_g \gg 1$ ), the scattering by the aggregates becomes predominant, and the structure factor depends on the fractal dimension of the aggregates (power-law regime). The change of the slope (in a log-log plot) takes place for intermediate values of  $q$  ( $qR_g \approx 1$ ), in the so-called Guinier regime (see Section 3).

The calculation of the fractal dimension implies then the plot in a log-log scale of the structure factor against the scattering wave vector. The fractal dimension can be directly obtained as the slope of the straight line in the power-law regime. Additionally, the radius of gyration can also be calculated by the plot of  $1/S(q)$  (calculated as  $I_0/I$ ) versus  $q^2$ , where the slope is found to be equal to  $R_g^2/3$ . This method has been applied in this work using the values of  $I$  obtained during the measurements performed with a Mastersizer 2000 (Malvern) instrument (see Section 3).

Dry fumed silica powder was fed to the Mastersizer 2000 using the Scirocco 2000M Manual Dry Powder Feeder, which is based on the free-fall of the powder from a hopper and re-entrainment by an air flow.

### 2.2. Fractal dimension by image analysis of SEM photographs

This method [5] uses the projected images of a large number of aggregates obtained by scanning electron microscope (SEM). SiO<sub>2</sub> powder has been dropped from a silo and collected by an electric low pressure impactor, ELPI [6,7] as described by [3]. In the ELPI, particles are classified and collected onto different stages, depending on their aerodynamic diameter. Nuclepore track-etched polycarbonate filters were placed on the ELPI stages, and the particles and agglomerates collected on the different stages were visualized by SEM, after platinum coating (coats 0.4–1 nm thick) and using a voltage of 5.0 kV. The agglomerates images were selected by changing the field of view and following random trajectories on the filter; several agglomerates in each field of view have been pictured, aiming to reduce operator bias. Magnification (from 5000 to 300,000, depending on the agglomerate size) was chosen to allocate an individual agglomerate to a maximum scan area.

The images, initially with 256 grey levels and 1280\*1024 pixels in size, are then binarised by manually selecting brightness thresholds to ascertain the entire aggregate. The 2D fractal dimension  $D_{f,2}$  is then derived as the slope on a least square linear fit of the plot of  $\log n$  versus  $\log$  (box size), where  $n$  is the number of non-overlapping equal boxes that would fill the projected surface area of the aggregate. All this operation can be carried out by the ImageJ software package,

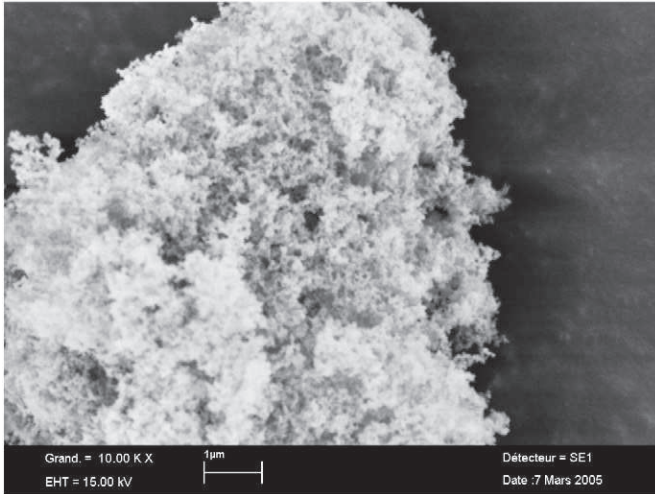


Fig. 1. SEM photograph of a fumed silica aggregate.

freely available at <http://rsb.info.nih.gov/ij/>. Aiming to take into account particle overlapping when observing an agglomerate, the 2D fractal dimension is then converted to a 3D fractal dimension  $D_{f,3}$  by multiplying  $D_{f,2}$  by 1.1 [2].

This method is only available for open aggregates ( $D_{f,2} < 2$ ). For more compact (and large) aggregates, computer simulations show that the 3D fractal dimension can be obtained from the perimeter fractal dimension,  $D_p$  [8,9]:

$$D_p = \begin{cases} 1 + (3 - D_{f,3})^{3/2} & \text{for } D_{f,3} \geq 2 \\ D_{f,3} & \text{for } D_{f,3} < 2 \end{cases} \quad (7)$$

$D_p$  is the fractal dimension of the perimeter of the aggregate. This fractal dimension is obtained in a similar way as  $D_{f,2}$ , but using only the perimeter of the particle.

The radius of gyration can be obtained by discretizing Eq. (3), [2]:

$$R_g^2 = G_{\text{tot}}^{-1} \sum_{x,y} G(x,y) [\mathbf{r}(x,y) - \mathbf{r}_{\text{cm}}]^2 \quad (8)$$

where  $G(x,y) = 0$  or 1 is the grey level of the pixel at position  $(x,y)$ , and  $G_{\text{tot}}$  the total grey level of the aggregate,

$$G_{\text{tot}} = \sum_{x,y} G(x,y) \quad (9)$$

and  $\mathbf{r}_{\text{cm}}$  is the position of the centre of mass of the aggregate.

$$\mathbf{r}_{\text{cm}} = G_{\text{tot}}^{-1} \sum_{x,y} G(x,y) \mathbf{r}(x,y) \quad (10)$$

### 3. Results and analysis

In this section the two previously presented methods are used to calculate the fractal dimension of the aggregates of fumed silica (Aerosil 200, Degussa).

#### 3.1. Fractal dimension by static light scattering (SLS)

Fig. 2 shows the classical plot of the structure factor versus the scattering wave vector for Aerosil 200. This result was obtained from measurements with a Mastersizer Malvern apparatus ( $\lambda = 632$  nm). The three regimes (Rayleigh, Guinier and power-law regimes) are clearly identified. First, the radius of gyration is calculated from the slope of the plot of  $I(0)/I$  versus  $q^2$  (Fig. 3) by rearranging Eq. (5) into

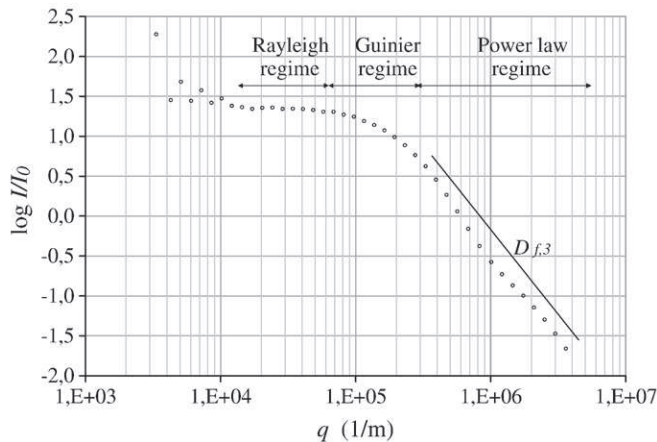


Fig. 2. SLS plot (structure factor versus scattering wave vector) for fumed silica aggregates.

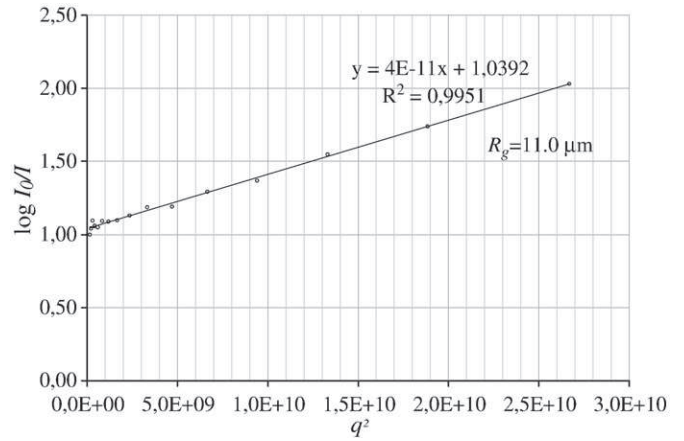


Fig. 3. Getting the radius of gyration by SLS. The slope of the plot of  $I_0/I$  versus  $q^2$  is equal to  $R_g^2/3$ . The scattering wave vector  $q$  is expressed in  $\text{m}^{-1}$ .

Eq. (11). Then the radius of gyration of the aggregates of fumed silica is found to be equal to  $11.0 \mu\text{m}$ .

$$[S(q)]^{-1} = \frac{I(0)}{I(q)} = 1 + \frac{1}{3} q^2 R_g^2 \quad \text{for } qR_g \approx 1 \quad (11)$$

Eq. (5) can be rearranged into Eq. (11), by considering that  $1 - x$  and  $1/(1+x)$  are similar functions with the same first-order Taylor development for small  $x$  values. Hence  $1 - (1/3)q^2 R_g^2$  can be approached as  $(1 + (1/3)q^2 R_g^2)^{-1}$ . Regression of  $I(0)/I(q)$  vs.  $q$  instead of  $I(q)/I(0)$  is preferable in view of the more important noise for very small scattering angles, as can be seen in Fig. 2. Hence, representing  $I(0)/I(q)$  seems a smarter approach, since the more noised value is kept in the numerator. Note that  $\exp(-x)$  has also the same first-order Taylor development, which explains why representing  $\ln(S(q))$  vs.  $q^2$  is sometimes found on the literature.

The fractal dimension  $D_{f,3}$  is then obtained as the slope of the log-log plot of  $I(0)/I$  versus  $qR_g$  (Fig. 4). The fractal dimension of the fumed silica aggregates is then 2.09. This fractal dimension is the averaged value of the fractal dimension of all the aggregates.

#### 3.2. Fractal dimension by image analysis of SEM photographs

The fractal dimension of several silica aggregates has been determined by image analysis of the SEM photographs of these aggregates. The results are reported on Fig. 5. Three regimes are observed. For very small aggregates, the number of primary particles in the aggregate is too small, and hence the definition of fractal

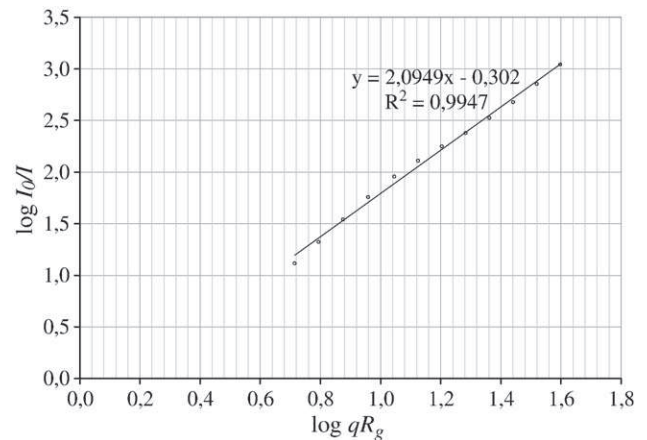


Fig. 4. Getting the fractal dimension by SLS. The slope of the plot of  $\log I_0/I$  versus  $\log qR_g$  is equal to  $D_{f,3}$ .

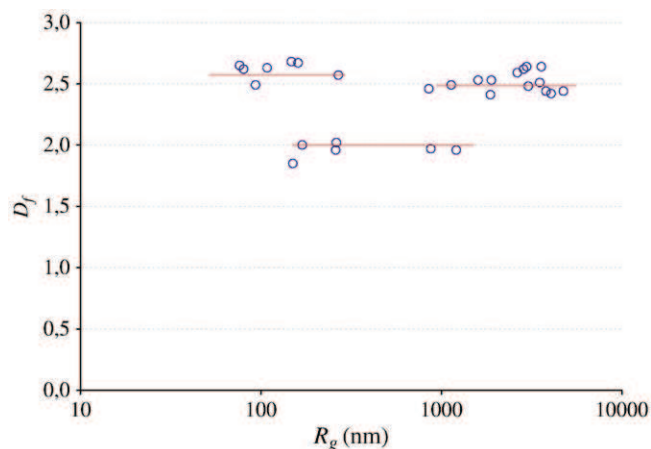


Fig. 5. Fractal dimension of the silica aggregates versus the radius of gyration of the aggregate.

dimension can not be used. For intermediate aggregates ( $R_g$  values comprised between 100 nm and 1  $\mu\text{m}$ ), the structure is quite open with a fractal dimension close to 2.0. Finally, big aggregates have a much more compact structure ( $D_{f,3} \approx 2.5$ ). Hence, it can be deduced that fumed silica has a two-level structure, which could be organized as shown in Fig. 6.

#### 4. Discussion and conclusions

SEM image analysis has shown that fumed silica aggregates have two different fractal dimensions, corresponding to a two-level structure. Hence, fumed silica is not really a mathematical fractal, which should have only one fractal dimension, aiming to be scale-invariant. Moreover, previous works have shown that agglomerates usually have a complex structure, with different compaction at different scales and hence different fractal dimensions [10–12]. This is not surprising, since agglomeration is driven by different phenomena at different scales [13]: Brownian motion for nanoparticles smaller than the Batchelor scale, laminar motion inside an eddy for aggregates between the Batchelor and the Kolmogorov scales, turbulent unsteady motion for aggregates bigger than the Kolmogorov scale. Hence, fractal dimension is rather a tool which leads to a simple description of the agglomerate structure (even for complex agglomerates).

The comparison of the results obtained by the two different methods shows that SLS does not give as much information as the

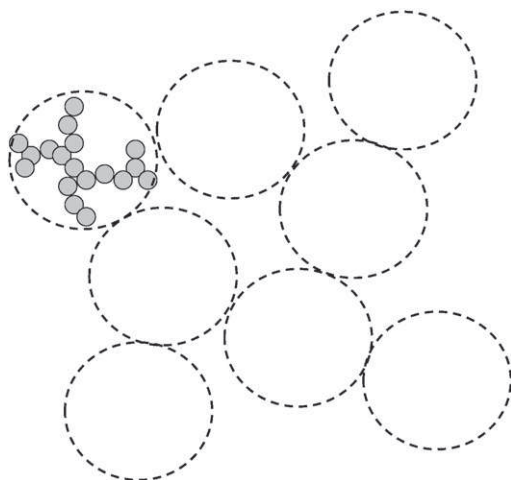


Fig. 6. Typical two-level structure (such as those of fumed silica), where aggregates have an open structure and then agglomerate in a much more compact way.

image analysis. First, only an averaged fractal dimension is obtained, and hence it is not possible to have any idea of a possible dispersion in the values of  $D_{f,3}$ . Secondly, only one fractal dimension has been detected. In fact, one of the fractal dimensions corresponds to a very small radius of gyration (between 100 and 1000 nm). It should be necessary to measure  $S(q)$  for very large values  $qR_g$ , not available by light scattering, even for very large scattering angles. Large values of  $q$  can be accessed by using X-rays scattering. However, X-rays scattering is a more unusual measuring device, much less used than SLS, which is commonly used in powder technology. Moreover, the two populations (aggregates and superaggregates) have too closed values of radius of gyration, which introduces a bias in the obtained values of the fractal dimension (and that, even if X-ray scattering would be used).

Two different methods have been used to characterize the fractal dimension of fumed silica aggregates. Although the image analysis is very time-consuming, it allows a much better characterization of the fractal dimension. Moreover, it enables to have the fractal dimension in specific cases, where the aggregates have very complex structures, such as 2-level structures. Static light scattering could be less accurate, although it remains a useful technique in some simple cases, due to its quickness.

#### Nomenclature

$a$	primary particle radius
$C$	proportionality constant
$C_p$	polydispersity factor
$D_f$	fractal dimension
$G$	grey level
$G_{\text{tot}}$	total grey level of the aggregate
$I$	intensity of the scattered light
$k_0$	proportionality constant
$n_{\text{pp}}$	number of primary particles
$q$	scattering wave vector
$r$	position
$r$	position of the centre of mass
$R_g$	radius of gyration
$S$	Structure factor
$\varepsilon$	agglomerate porosity
$\lambda$	wavelength
$\rho$	density

#### Acknowledgements

Authors are sincerely acknowledged to Stéphane Le Blond du Plouy (TEMSCAN Service of the Paul University of Toulouse), for all the images obtained by SEM in the frame of this work. The CNRS (French National Scientific Research Centre) and the INRS (French National Institute for Research and Security) are also acknowledged, for their financial support in the framework of the ACI DINANO project (2004–2007).

#### References

- [1] H. Brune, H. Ernst, A. Grünwald, W. Grünwald, H. Hofmann, H. Krug, P. Janich, M. Mayor, W. Rathgeber, G. Schmid, U. Simon, V. Vogel, D. Wyrwa, Nanotechnology, Assessment and Perspectives, Springer, Berlin Heidelberg, 2006.
- [2] P.A. Baron, C.M. Sorensen, J.E. Brockmann, Nonspherical particle measurement: shape factors, fractals, and fibers, in: P.A. Baron, K. Willeke (Eds.), Aerosol Measurement. Principles, Techniques, and Applications, 2nd edition, Wiley-Interscience, Hoboken, 2001.
- [3] N. Ibaseta, B. Biscans, Ultrafine aerosol emission from free-fall of  $\text{TiO}_2$  And  $\text{SiO}_2$  nanopowders, KONA 25 (2007) 190–204.
- [4] C.M. Sorensen, Light scattering by fractal aggregates: a review, Aerosol Sci. Technol. 35 (2) (2001) 648–687.
- [5] P. Gwaze, O. Schmid, H.J. Annegarn, M.O. Andrae, J. Huth, G. Helas, Comparison of three methods of fractal analysis applied to soot aggregates from wood combustion, J. Aerosol Sci. 37 (7) (2006) 820–838.

- [6] J. Keskinen, K. Pietarinen, M. Lehtimäki, Electrical low pressure impactor, *J. Aerosol Sci.* 23 (1992) 353–360.
- [7] M. Marjamäki, J. Keskinen, D.-R. Chen, D.Y.H. Pui, Performance evaluation of the electrical low-pressure impactor (ELPI), *J. Aerosol Sci.* 31 (2000) 249–261.
- [8] R. Jullien, R. Thouy, F. Ehrburger-Dolle, Numerical investigation of two-dimensional projections of random fractal aggregates, *Phys. Rev. E* 50 (5) (1994) 3878.
- [9] R. Dhaubhadel, F. Pierce, A. Chakrabarti, C.M. Sorensen, Hybrid superaggregate morphology as a result of aggregation in a cluster-dense aerosol, *Phys. Rev. E* 73 (1) (2006) 011404.
- [10] A. Eshuis, C.A.J. Koning, The mechanism of particle formation during homogeneous precipitation of zinc sulphide, *Colloid Polym. Sci.* 272 (10) (1994) 1240–1244.
- [11] A. Eshuis, G.R.A. van Elderen, C.A.J. Koning, A descriptive model for the homogeneous precipitation of zinc sulphide from acidic zinc salt solutions, *Colloid Surf. A* 151 (3) (1999) 505–512.
- [12] W. Kim, C.M. Sorensen, D. Fry, A. Chakrabarty, Soot aggregates, superaggregates and gel-like networks in laminar diffusion flames, *J. Aerosol Sci.* 37 (5) (2006) 386–401.
- [13] R. David, F. Espitalier, A. Cameirão, L. Rouleau, Developments in the understanding and modeling of the agglomeration of suspended crystals in crystallization from solutions, *KONA* 21 (2003) 40–53.